Cancer Cell
Article

Myeloid Leukemia Development in c-Cbl RING Finger Mutant Mice Is Dependent on FLT3 Signaling

Chozhavendan Rathinam,[1,4] Christine B.F. Thien,[2,4] Richard A. Flavell,[1,3,*] and Wallace Y. Langdon[2,*]
[1]Department of Immunobiology, Yale University School of Medicine, New Haven, CT 06510, USA
[2]School of Pathology and Laboratory Medicine, University of Western Australia, Crawley, WA 6009, Australia
[3]Howard Hughes Medical Institute, New Haven, CT 06520, USA
[4]These authors contributed equally to this work
*Correspondence: richard.flavell@yale.edu (R.A.F.), wally.langdon@uwa.edu.au (W.Y.L.)
DOI 10.1016/j.ccr.2010.09.008

SUMMARY

Although myeloid leukemias are primarily caused by leukemic stem cells, the molecular basis of their transformation remains largely unknown. Here, by analyzing mice with a mutation in the RING finger domain of c-Cbl, we show that the E3 ubiquitin ligase activity of c-Cbl is required to restrict myeloid leukemia development. These mice develop a myeloproliferative disease which progresses to leukemia and involves hematopoietic progenitors that exhibit augmented FLT3 signaling. Suppressing this signaling through matings with FLT3 ligand knockout mice prevents leukemia development. We also observe enhanced c-Kit, Akt and Erk activity, and deregulated expression of leukemia-associated transcription factors in hematopoietic progenitors. The characterization of these perturbations provides direction for therapeutics that may aid the treatment of patients with c-Cbl mutations.

INTRODUCTION

c-*Cbl* (Casitas B cell lymphoma), the cellular homolog of the v-*Cbl* oncogene (Langdon et al., 1989), encodes a RING finger-based E3 ubiquitin ligase that negatively regulates the activity of many signaling pathways (Thien and Langdon, 2005). This regulation is achieved by targeting an array of growth factor receptors, antigen receptors, and protein tyrosine kinases, thereby directing their polyubiquitylation and degradation. c-Cbl also functions as a multidomain adaptor that recruits signaling proteins such as phosphatidylinositol 3-kinase (PI3K) and Crk. Indeed c-Cbl is probably the most extensively studied E3 ubiquitin ligase and has been shown to be involved in the regulation of ~150 cellular proteins, either directly or indirectly (Schmidt and Dikic, 2005).

Although the biochemistry of c-Cbl's E3 ligase activity and its molecular interactions have been well characterized, the in vivo roles of c-Cbl in hematopoiesis and leukemogenesis remain elusive. Understanding this has become increasingly important with the widespread involvement of mutated forms of c-Cbl in human myeloproliferative neoplasms (MPNs) (Dunbar et al., 2008; Grand et al., 2009; Loh et al., 2009; Makishima et al., 2009; Muramatsu et al., 2010; Sanada et al., 2009). Patients examined to date number approximately 1800 and the MPNs include myelodysplastic syndromes (MDS) and MDS/myeloproliferative disease (MPD) overlap entities chronic myelomonocytic leukemia (CMML) and juvenile myelomonocytic leukemia (JMML), atypical chronic myeloid leukemia, myelofibrosis, and secondary acute myeloid leukemia (AML). The incidence of c-Cbl mutations in MPDs is between 5% and 15%, with the highest rates occurring in CMML and JMML (for review, see Kales et al., 2010; Ogawa et al., 2010). These studies relied on single nucleotide polymorphism (SNP) array karyotyping to detect regions of acquired uniparental disomy (aUPD), a somatic chromosomal aberration that results in copy-neutral loss of heterozygosity (Maciejewski et al., 2009). A common region of aUPD was found to involve chromosome 11q focusing attention on c-*Cbl* which is located at 11q23.3. DNA sequencing showed that 80%–100% of patients with 11q aUPD carried homozygous c-*Cbl* mutations located in, or spanning, the linker and RING finger domains that are essential for interactions with E2 ubiquitin conjugating enzymes (Zheng et al., 2000).

Significance

The c-*Cbl* proto-oncogene is mutated in a wide range of human myeloproliferative neoplasms. Through analysis of a c-Cbl RING finger mutant mouse, we show that the E3 ubiquitin ligase activity of c-Cbl is critical for suppressing myeloid proliferation and the development of leukemia. This mouse therefore provides a model for studying the progression of c-Cbl-associated leukemogenesis and the identification of cooperative mutations. Furthermore, this preclinical model provides an avenue for testing the efficacy of therapeutic agents that target signaling molecules activated by oncogenic forms of c-Cbl.

Recently, we found c-Cbl to be highly expressed in hematopoietic stem cells (HSCs) and, through the analysis of c-Cbl mutant mice, identified c-Cbl to be a critical negative regulator of HSC function (Rathinam et al., 2008; Yokomizo and Dzierzak, 2008). These observations suggest that perturbations affecting this regulatory role could promote the development of hematopoietic neoplasms. Here, we test this possibility by examining knockin mice with loss-of-function mutations in the RING finger domains of c-Cbl and Cbl-b, a homolog with a high level of identity to c-Cbl (Oksvold et al., 2008; Thien et al., 2005). The mutation in these mice is a substitution of an alanine for the N-terminal cysteine in the C_3HC_4 RING domain, positioned at 379 in c-Cbl (i.e., C379A) and 373 in Cbl-b (i.e., C373A), that disrupts the interaction with E2 conjugating enzymes therefore abolishing E3 ubiquitin ligase activity. In this study, we examined c-Cbl and Cbl-b RING finger knockin mice, and their respective knockouts, to determine whether any of these mutations promote the development of hematopoietic neoplasms.

RESULTS

MPD in Young c-Cbl Mutant Mice

To understand the functions of Cbl proteins in hematopoiesis and leukemogenesis, we made use of c-Cbl and Cbl-b knockout-mice (i.e., c-Cbl$^{-/-}$ and Cbl-b$^{-/-}$), and two mutant RING finger knockins, i.e., c-Cbl(C379A) and Cbl-b(C373A). c-Cbl$^{-/-}$, Cbl-b$^{-/-}$, and Cbl-b(C373A) mice breed successfully as homozygous mutants, whereas analysis of c-Cbl(C379A) knockin mice requires the generation of mice with a single mutated RING finger allele and a null allele as most homozygous c-Cbl RING finger mutant mice die in utero (Thien et al., 2005). These single copy mutant mice, termed c-Cbl$^{A/-}$, are generated from matings between c-Cbl$^{-/-}$ x c-Cbl$^{A/+}$ mice. In this study, we use c-Cbl$^{+/-}$ littermates, aged matched wild-type (WT) c-Cbl$^{+/+}$ mice, or heterozygous c-Cbl$^{A/+}$ mice as controls.

Analysis of bone marrow (BM) from 8-week-old Cbl mutant mice revealed an expansion in the frequency of myeloid lineage cells in c-Cbl$^{-/-}$ and c-Cbl$^{A/-}$ mice which was not present in either the Cbl-b$^{-/-}$ mouse or the Cbl-b RING finger knockin (Cbl-b$^{A/A}$). This was evident by the greater proportion of CD11b$^+$ and Gr-1$^+$ cells in the BM from both the c-Cbl mutants, which was accompanied by a decrease in the numbers of red blood cells (RBCs) and B-lineage cells (Figure 1A; data not shown).

A consequence of the myeloid expansion in the marrow is a splenic disorder in c-Cbl$^{-/-}$ and c-Cbl$^{A/-}$ mice characterized by increased hematopoiesis with an expanded red pulp caused by increased numbers of infiltrating RBCs, monocytes, granulocytes, and megakaryocytes (Figure 1B). However, the disruption to splenic architecture and splenomegaly is clearly more pronounced in c-Cbl$^{A/-}$ mice compared with c-Cbl$^{-/-}$ mice (Figures 1B and 1C), suggesting that additional signaling perturbations, beyond the loss of c-Cbl E3 ligase activity, are affecting hematopoiesis in this mouse. In contrast Cbl-b mutant mice had WT levels of BM cell populations and structurally normal splenic follicles and red pulp (Figures 1A and 1B).

Although c-Cbl$^{-/-}$ mice develop a mild myeloproliferative disorder (Murphy et al., 1998; Naramura et al., 1998; Sanada et al., 2009; Thien et al., 2003), these animals fail to progress to a severe myeloid disease, even at later stages (~2 years) of life. In addition, neither Cbl-b$^{-/-}$ nor Cbl-b RING finger mutant mice develop any signs of hematologic proliferative disorders as they age. In contrast survival of c-Cbl$^{A/-}$ mice was significantly reduced through the development of myeloid leukemia. Cohorts of c-Cbl$^{A/-}$ and c-Cbl$^{+/-}$ littermates were therefore established for a detailed characterization of the disease.

Leukemia Development in c-Cbl RING Finger Mutant Mice

All Cbl$^{A/-}$ mice in a cohort of 28 mice developed an aggressive myeloid leukemia with the majority of mice succumbing within the first year of life (Figure 2A). All mice show marked splenomegaly and significantly elevated white blood cell (WBC) counts compared with their c-Cbl$^{+/-}$ littermates (Figures 2B and 2C). Blood films and flow cytometry revealed a marked increase in the numbers of promonocytes, monocytes, neutrophils, and, to varying degrees, B lymphocytes (Figure 2E; Figure S1). The B cell expansion, however, was not evident in the BM or spleen (Figure S1), nor did the B-lineage cells invade the liver, kidneys, or lungs where myeloid cells predominated. An example of a leukemic c-Cbl$^{A/-}$ mouse is shown in Figure 2D. This mouse showed an increase in the numbers of monocytes, neutrophils and B lymphocytes in the blood (Figure 2E; Figure S1 see mouse F10) and an extensive infiltration of monocytes into the spleen, liver, kidney and lungs (Figure 2F). Immunophenotyping of BM, spleen and blood confirmed the expansion of CD11b$^+$ and Gr-1$^+$ cells (Figure 2G). In the spleen and BM this was accompanied by a marked reduction in IgD$^+$ B cells and an increase in the proportion of immature CD19$^+$ IgD$^-$ cells in the spleen (Figure 2G). A CD11b$^+$ CD19$^+$ population was also evident in the blood, and to a lesser extent in the spleen, of some of the leukemic mice (Figure 2G; Figure S1). This phenotype has been observed in a subclass of aggressive human acute leukemias (Owaidah et al., 2006). Approximately half the mice also exhibited varying degrees of lymph node involvement due to an expansion of large B-lineage cells (Figures S1C and S1D). These phenotypic characterizations indicate the existence of leukemic progenitors capable of differentiating along myeloid or B-lineage pathways. However, this bipotential was only evident in blood and lymph nodes whereas the splenic and BM environments promoted the expansion of myeloid lineage cells. Furthermore, unlike v-Cbl-induced malignancies (Langdon et al., 1989), no mice solely developed pre-B cell lymphomas.

A number of studies have found heterozygous c-Cbl mutations in AML patients (Abbas et al., 2008; Caligiuri et al., 2007; Masashi et al., 2008; Reindl et al., 2009; Rodrigues et al., 2008; Sargin et al., 2007); however, while c-Cbl$^{A/+}$ mice examined at 20–30 weeks of age showed mild signs of increased intrasplenic hematopoiesis, none progressed to develop leukemia (data not shown). The reason why heterozygous c-Cbl mutations can contribute to the development of AML in humans, but not mice, is not known; however, in most cases the human mutations involve exon 8 or exon 8/9 deletions which have been found to have enhanced oncogenic potential compared with point mutations in the RING finger domain (Bandi et al., 2009; Reindl et al., 2009; Thien et al., 2001). Furthermore, a heterozygous exon 8 deletion in c-Cbl has been identified in a *NUP98-HOXD13* transgenic model of MDS that progressed to AML (Slape et al., 2008).

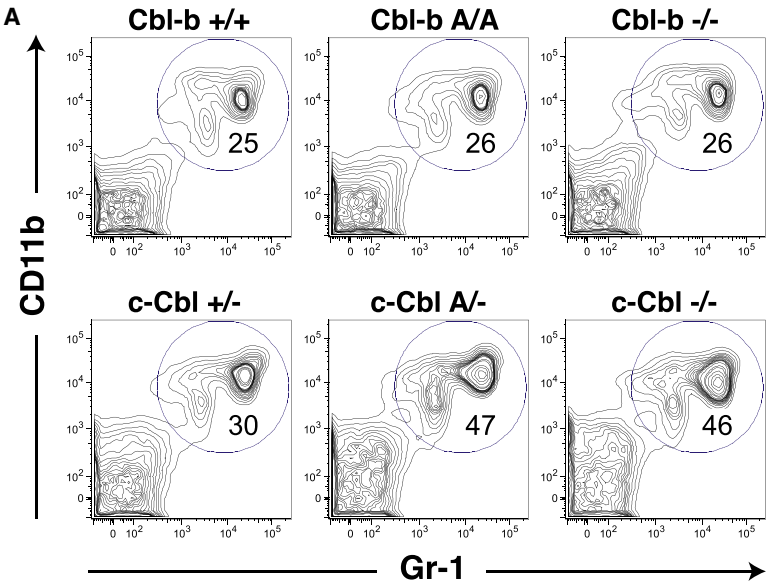

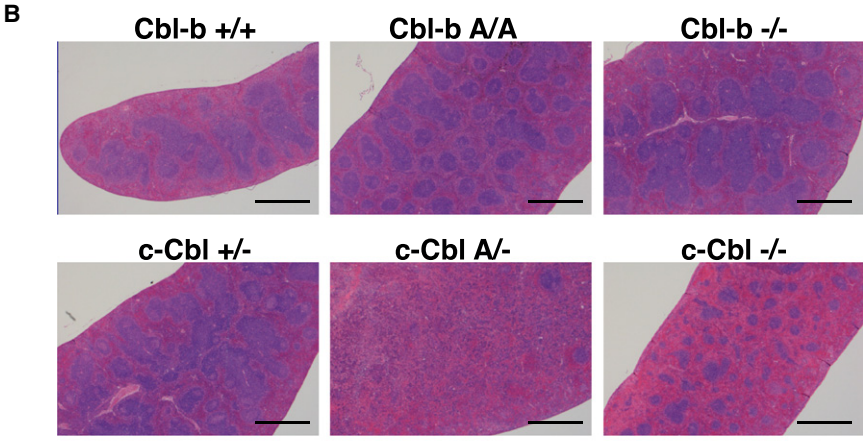

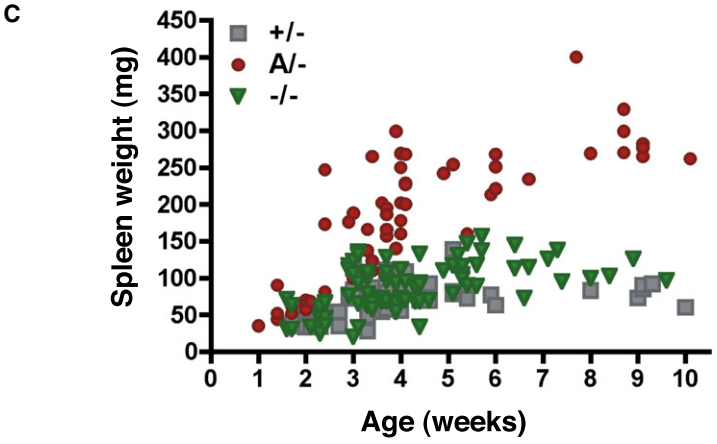

Figure 1. Young Preleukemic c-Cbl Mutant Mice Show an Expanded Population of Myeloid Lineage Cells in Their Bone Marrow and Increased Intrasplenic Hematopoiesis

(A) Bone marrow from 8-week-old Cbl-b WT (Cbl-b$^{+/+}$), Cbl-b(C373A) RING finger knockin mutant (Cbl-b$^{A/A}$), Cbl-b knockout (Cbl-b$^{-/-}$), c-Cbl heterozygous knockout (c-Cbl$^{+/-}$), c-Cbl(C379A) RING finger knockin mutant (c-Cbl$^{A/-}$), and c-Cbl knockout (c-Cbl$^{-/-}$) mice were analyzed for myeloid lineage cells by anti-CD11b and anti-Gr-1 antibody staining and flow cytometry. Data are representative of five independent experiments.

(B) H&E-stained sections of spleens from young mice (9–13 weeks) of the same genotypes as above. The spleens from both c-Cbl mutant mice show a disrupted architecture due to an expansion of the red pulp which can be seen infiltrating the splenic follicles. Scale bars, 1mm.

(C) Marked splenic enlargement in young c-Cbl RING finger mutant mice (A/–) compared with WT littermates (+/–) and c-Cbl knockout mice (–/–).

This finding suggests that heterozygous c-Cbl mutations may be more effective in promoting leukemogenesis when cells have acquired an initiating mutation.

c-Cbl RING Finger Mutant LT-HSCs Transfer MPD, and Leukemic Phenotypes

A hallmark of leukemia initiating cells is the ability to transfer the disease upon transplantation into irradiated WT recipient mice (Bonnet, 2005; Lapidot et al., 1994; Wang and Dick, 2005). Therefore, to address whether the MPD and leukemic phenotypes of c-Cbl$^{A/-}$ mice are transferable and cell intrinsic BM transplantation studies were performed using donor cells from preleukemic mice. Three months after transplantation recipient mice receiving c-Cbl$^{A/-}$ BM cells showed evidence of myeloid leukemia development (Figure 3A). To identify which hematopoietic populations are required for leukemia development, we isolated BM cells representing various developmental stages of myelopoiesis from 8-week-old c-Cbl$^{A/+}$ and c-Cbl$^{A/-}$ mice. These cells were then transplanted into sublethally irradiated *RAG2*-deficient congenic recipient mice, as described earlier (Passegue et al., 2004). While unfractionated total BM cells always transferred the disease, c-Kit-depleted BM did not, suggesting that the leukemia initiating cells reside in the hematopoietic progenitor compartment (Figure 3B). Transfer of common myeloid progenitor (CMP), granulocyte myeloid progenitor (GMP), CMP + GMP + megakaryocyte erythrocyte progenitor (MEP), Gr1^{+}CD11b^{+} cells, and splenocytes also did not result in the development of leukemia (Figure 3B), although donor-derived

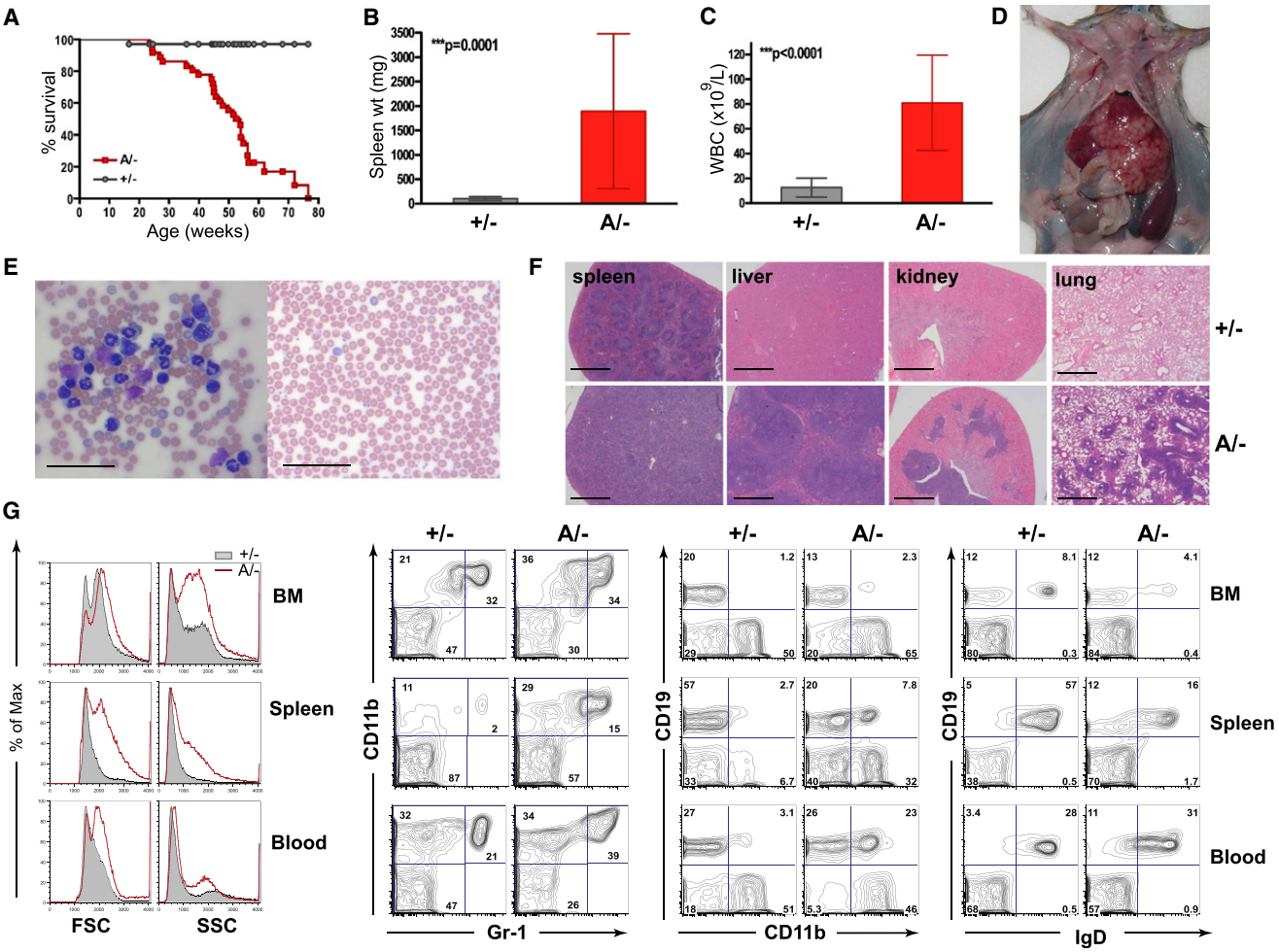

Figure 2. Characterization of c-Cbl$^{A/-}$ Leukemic Mice

(A) Kaplan-Meier survival plot showing reduced survival of c-Cbl$^{A/-}$ mice compared with their corresponding c-Cbl$^{+/-}$ normal littermates. The median survival of c-Cbl$^{A/-}$ mice was 47.5 weeks and the mean survival ± SD was 46.8 ± 13 weeks (n = 28).

(B) Spleen weights of c-Cbl$^{A/-}$ leukemic mice at the time of death compared with c-Cbl$^{+/-}$ littermate controls. Mean spleen weights ± SD are 103 ± 41 mg for c-Cbl$^{+/-}$ mice and 1896 ± 1578 mg for c-Cbl$^{A/-}$ mice (n = 20). p = 0.0001 by two-sided unpaired t test.

(C) Increased white blood cell (WBC) counts of c-Cbl$^{A/-}$ leukemic mice at the time of death compared with c-Cbl$^{+/-}$ littermates. Mean WBC counts ± SD are 12 ± 7 × 10^9/liter for c-Cbl$^{+/-}$ mice and 81 ± 38 × 10^9/liter for c-Cbl$^{A/-}$ mice (n = 20). p < 0.0001 by two-sided unpaired t test.

(D) Photograph of a representative c-Cbl$^{A/-}$ leukemic mouse that succumbed to myeloid leukemia at 44 weeks of age. Note the splenomegaly and extensive infiltration of leukemic cells into the liver. Enlarged inguinal and cervical lymph nodes are also evident.

(E) Diff-Quick stained blood smears showing monocytes, neutrophils, and lymphocytes in the blood from the 44-week-old c-Cbl$^{A/-}$ leukemic mouse shown in (D) compared with its c-Cbl$^{+/-}$ normal littermate. Scale bar, 50μm.

(F) H&E stained tissue sections of spleen, liver, kidney, and lung from the c-Cbl$^{A/-}$ leukemic mouse shown in (D) showing extensive infiltration of leukemic cells compared with its c-Cbl$^{+/-}$ littermate. Scale bar, 1mm.

(G) Immunophenotyping of a c-Cbl$^{A/-}$ leukemic mouse and its c-Cbl$^{+/-}$ littermate. Bone marrow (BM), spleen, and blood cells from a 44-week-old c-Cbl$^{A/-}$ leukemic mouse and its c-Cbl$^{+/-}$ littermate were analyzed by flow cytometry to determine forward and side scatter profiles and the proportions of CD11b$^+$,Gr-1$^+$; CD11b$^+$,CD19$^+$, and CD19$^+$,IgD$^+$ cells. See also Figure S1.

(CD45.2$^+$) hematopoiesis could be detected after 4 weeks of transplantation (Figure S2). These results suggested that MPD and leukemia development is dependent on the presence of progenitors before the CMP stage. Interestingly, analysis of recipients transferred with either long-term HSCs (LT-HSCs) or short-term HSCs (ST-HSCs) + multipotent progenitors (MPPs) revealed that the leukemia initiating cells requires the LT-HSC compartment since it was only recipients that received LT-HSCs from c-Cbl$^{A/-}$ mice that developed MPD and progressed to leukemia (Figure 3B). The inability of ST-HSCs and MPPs to transfer the disease was not due to a lack of repopulating ability as donor-derived myeloid lineage cells could still be detected up to 6 months posttransplantation (Figure S2). In contrast, no recipient mice that received LT-HSCs from heterozygous c-Cbl$^{A/+}$ mice developed MPD or leukemia (Figure 3B). Equivalent results were obtained when hematopoietic fractions from 40-week-old leukemic c-Cbl$^{A/-}$ mice were transplanted into sublethally irradiated *RAG2*-deficient recipients (Figure 3C),

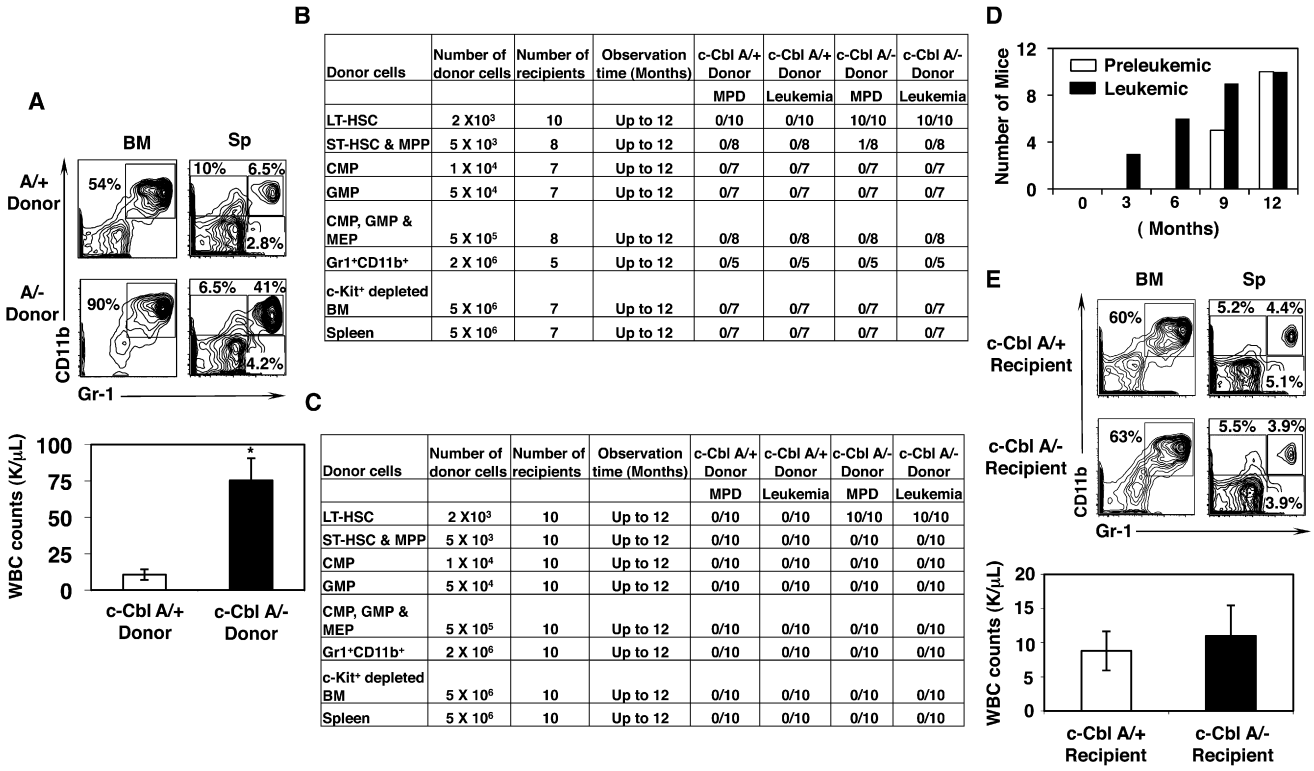

B

Donor cells	Number of donor cells	Number of recipients	Observation time (Months)	c-Cbl A/+ Donor	c-Cbl A/+ Donor	c-Cbl A/- Donor	c-Cbl A/- Donor
				MPD	Leukemia	MPD	Leukemia
LT-HSC	2 X10^3	10	Up to 12	0/10	0/10	10/10	10/10
ST-HSC & MPP	5 X 10^3	8	Up to 12	0/8	0/8	1/8	0/8
CMP	1 X 10^4	7	Up to 12	0/7	0/7	0/7	0/7
GMP	5 X 10^4	7	Up to 12	0/7	0/7	0/7	0/7
CMP, GMP & MEP	5 X 10^5	8	Up to 12	0/8	0/8	0/8	0/8
Gr1$^+$CD11b$^+$	2 X 10^6	5	Up to 12	0/5	0/5	0/5	0/5
c-Kit$^+$ depleted BM	5 X 10^6	7	Up to 12	0/7	0/7	0/7	0/7
Spleen	5 X 10^6	7	Up to 12	0/7	0/7	0/7	0/7

C

Donor cells	Number of donor cells	Number of recipients	Observation time (Months)	c-Cbl A/+ Donor	c-Cbl A/+ Donor	c-Cbl A/- Donor	c-Cbl A/- Donor
				MPD	Leukemia	MPD	Leukemia
LT-HSC	2 X10^3	10	Up to 12	0/10	0/10	10/10	10/10
ST-HSC & MPP	5 X 10^3	10	Up to 12	0/10	0/10	0/10	0/10
CMP	1 X 10^4	10	Up to 12	0/10	0/10	0/10	0/10
GMP	5 X 10^4	10	Up to 12	0/10	0/10	0/10	0/10
CMP, GMP & MEP	5 X 10^5	10	Up to 12	0/10	0/10	0/10	0/10
Gr1$^+$CD11b$^+$	2 X 10^6	10	Up to 12	0/10	0/10	0/10	0/10
c-Kit$^+$ depleted BM	5 X 10^6	10	Up to 12	0/10	0/10	0/10	0/10
Spleen	5 X 10^6	10	Up to 12	0/10	0/10	0/10	0/10

Figure 3. Leukemia in c-Cbl Mutant Mice Is an HSC Disorder

(A) RBC-depleted BM (1 × 10^6) cells from 8-week-old c-Cbl$^{A/+}$ and c-Cbl$^{A/-}$ mice (CD45.2$^+$) were injected into lethally irradiated 8-week-old WT CD45.1$^+$ congenic recipients. Three months after transplantation, donor-derived (CD45.2$^+$) cells from BM (left) and spleen (right) were gated and analyzed for CD11b and Gr1 expression. WBC counts in the peripheral blood (bottom) of recipient mice were measured and indicated (mean ± SD; n = 5). Data are representative of two independent experiments.

(B) Sublethally irradiated *RAG2*$^{-/-}$ CD45.1 recipient mice were injected with the indicated numbers of fractionated donor BM subsets or splenocytes isolated from 8-week-old c-Cbl$^{A/+}$ and c-Cbl$^{A/-}$ (preleukemic) mice. Recipients were monitored monthly for up to 12 months, starting at 4 weeks after transplantation, by flow cytometric and differential counts of peripheral blood. BM, spleen, liver, lungs, and kidneys were further analyzed by flow cytometry and histology to determine leukemia development. All the data shown here were generated from an individual experiment. The data points were collected from each mouse of the specified individual groups and presented. Data are representative of two independent experiments.

(C) Sublethally irradiated *RAG2*$^{-/-}$ CD45.1 recipient mice were injected with the indicated numbers of fractionated donor BM subsets or splenocytes isolated from 40-week-old c-Cbl$^{A/+}$ and c-Cbl$^{A/-}$ (leukemic) mice. Recipients were monitored monthly for up to 12 months to determine leukemia development. All the data shown here were generated from an individual experiment. The data points were collected from each mouse of the specified individual groups and presented. Data are representative of two independent experiments.

(D) A graph representing the kinetics of leukemia caused by the transfer of LT-HSCs obtained from 8-week-old preleukemic c-Cbl$^{A/-}$ mice (white bars) or 40-week-old leukemic mice (black bars). The data shown here were generated from an individual experiment and are representative of two independent experiments.

(E) BM cells (1 × 10^6) from 8-week-old WT congenic (CD45.1) mice were injected into lethally irradiated 8-week-old c-Cbl$^{A/+}$ and c-Cbl$^{A/-}$ (CD45.2) recipients. Three months after transplantation, donor-derived (CD45.1$^+$) cells of BM (left) and spleen (right) were gated and analyzed for CD11b and Gr1 expression. WBC counts in the peripheral blood (bottom) of recipient mice were measured and indicated (mean ± SD; n = 5). Data are representative of two independent experiments. See also Figure S2.

although the latency was reduced compared with mice receiving preleukemic LT-HSCs (Figure 3D).

These data provided proof that the leukemia initiating cells are present within the hematopoietic compartment of the BM; nevertheless, pre-exposure of hematopoietic cells to the c-Cbl mutant microenvironment might irreversibly alter their properties before transplantation. Indeed, recent studies have shown that myeloid leukemia can be caused by defects in the microenvironment (Raaijmakers et al., 2010; Walkley et al., 2007). To test this possibility, CD45.1 WT congenic BM cells were transplanted into lethally irradiated c-Cbl$^{A/-}$ and c-Cbl$^{A/+}$ recipients. Analysis after 12, 24, and 32 weeks of transplantation revealed no evidence of MPD or leukemia development in c-Cbl$^{A/+}$ and c-Cbl$^{A/-}$ recipients (Figure 3E; data not shown).

Enhanced Receptor Tyrosine Kinase (RTK) Signaling in Cbl$^{A/-}$ Hematopoietic Progenitors

c-Cbl is a negative regulator of RTK signaling through its E3 ubiquitin ligase activity and c-Cbl mutations found in human leukemias abolish this function (for review, see Kales et al., 2010; Ogawa et al., 2010). Since myeloid malignancies involving c-Cbl originate from hematopoietic precursors we focused on signaling by c-Kit and FLT3, and the roles they may play in promoting leukemia in c-Cbl$^{A/-}$ mice. To examine signaling

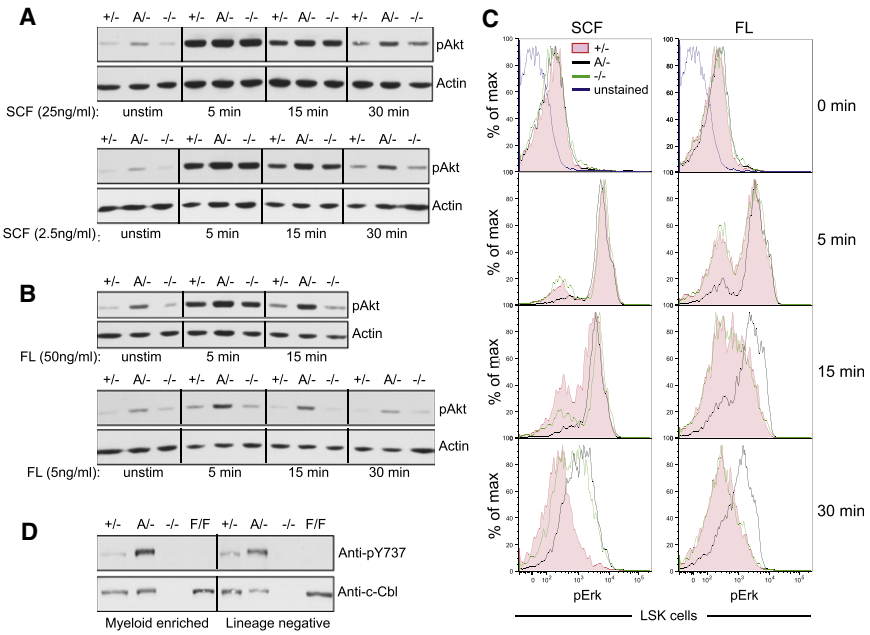

Figure 4. Constitutive Activation of Akt in Lineage-Negative Hematopoietic Cells from c-Cbl$^{A/-}$ Mice

(A and B) Lineage negative BM cells from 7-week-old c-Cbl$^{+/-}$, c-Cbl$^{A/-}$, and c-Cbl$^{-/-}$ mice were incubated in serum-free media for 1 hr at 37°C. The cells were either left unstimulated or stimulated at 37°C with SCF or FL at the concentrations and times indicated. The cells were lysed in SDS PAGE sample buffer and analyzed for the levels of phospho-Akt(S473) by immunoblotting. The blots were probed with anti-actin antibodies to indicate the relative protein levels in each track. Note the higher level of constitutively active Akt in cells from the c-Cbl RING finger mutant mouse which is sustained following SCF or FL stimulation. (C) FL- and SCF-stimulated LSK cells from c-Cbl$^{A/-}$ mice show sustained Erk activation. Lineage negative bone marrow cells stimulated with 25 ng/ml of SCF or 50 ng/ml of FL were stained with anti-c-Kit, -Sca-1 and -phospho-Erk antibodies and analyzed by flow cytometry. LSK cells from c-Cbl$^{A/-}$ and c-Cbl$^{-/-}$ mice show phospho-Erk levels that are sustained to equivalent levels following SCF stimulation, whereas FL stimulation revealed a markedly sustained signal unique to c-Cbl$^{A/-}$ cells.

(D) BM cells from c-Cbl$^{+/-}$, c-Cbl$^{A/-}$, c-Cbl$^{-/-}$, and c-Cbl$^{F/F}$ mice were enriched for myeloid lineage cells or lineage negative cells then incubated in serum-free media for 1 hr at 37°C before analysis by immunoblotting with anti-c-Cbl phospho-tyrosine 737 or anti-c-Cbl antibodies. Of note is the higher level of constitutively phosphorylated tyrosine 737 in the mutant RING finger protein compared with WT c-Cbl. Antibody specificity was confirmed by including cells from a mouse expressing a Y737F knockin mutation (i.e., F/F) that is not recognized by antiphospho-Y737 antibodies. See also Figure S3.

responses, we purified lineage negative (Lin$^-$) BM cells from young preleukemic c-Cbl$^{+/-}$, c-Cbl$^{A/-}$, and c-Cbl$^{-/-}$ mice and stimulated them with either stem cell factor (SCF) or FLT3 ligand (FL). Because of the marked activation of Akt in thymocytes from c-Cbl$^{A/-}$ mice, but not c-Cbl$^{-/-}$ mice (Thien et al., 2005, 2010), we initially examined the activity of Akt. Immunoblotting with anti-phospho-Akt antibodies revealed a higher level of constitutive Akt activation in serum-starved Lin$^-$ BM cells from c-Cbl$^{A/-}$ mice compared with both c-Cbl$^{+/-}$ and c-Cbl$^{-/-}$ mice (Figures 4A and 4B). Following stimulation with SCF, all three genotypes showed an equivalent induction of phospho-Akt, but the Akt signal was sustained in c-Cbl$^{A/-}$ cells (Figure 4A, see 30 min). This sustained signal does not appear to be due to either increased levels of c-Kit expression or a greater proportion of c-Kit-positive cells since they were similar among the three genotypes (Figure S3). Similar effects were seen following FL stimulation where c-Cbl$^{A/-}$ cells showed a more sustained activation of Akt (Figure 4B). The enhanced induction of phospho-Akt in c-Cbl$^{A/-}$ cells compared with both c-Cbl$^{+/-}$ and c-Cbl$^{-/-}$ cells was more marked when a suboptimal concentration (5 ng/ml) of FL was used suggesting a heightened sensitivity to FL-stimulation (Figure 4B, lower panel). This greater level of stimulation may in part be due to the presence of an expanded population of FLT3^{high} cells in c-Cbl$^{A/-}$ mice (Figure S3). This population is characterized in more detail in the subsequent section.

SCF and FL-induced activation of Erk was also analyzed, but in this case by flow cytometry which enabled the examination of LSK cells (Figure 4C). Unfortunately, attempts to detect phospho-Akt induction by flow cytometry were unsuccessful therefore restricting our Akt analysis to immunoblotting as described above. There was no detectable difference in constitutive phospho-Erk levels cells (Figure 4C, 0 min), and following 5 min of SCF stimulation a large but equivalent induction of Erk was observed in LSK cell from all three genotypes (Figure 4C). However by 30 min c-Cbl$^{A/-}$ and c-Cbl$^{-/-}$ LSK cells showed a more sustained signal compared with wild-type cells. This enhanced phospho-Erk signal in both c-Cbl mutants is consistent with our findings in thymocytes following T cell receptor stimulation (Thien et al., 2005). In contrast FL stimulation of LSK cells led to a sustained phospho-Erk signal that was only evident in c-Cbl$^{A/-}$ cells, whereas phospho-Erk levels in c-Cbl$^{+/-}$ and c-Cbl$^{-/-}$ LSK cells showed equivalent intensities and kinetics (Figure 4C). This finding, along with the greater responsiveness of c-Cbl$^{A/-}$ lineage negative cells to FL activation of Akt, provides evidence that heightened FLT3 signaling may be a contributing factor that distinguishes the c-Cbl$^{A/-}$ mouse from the c-Cbl$^{-/-}$ mouse in their contrasting susceptibilities to leukemia development.

Since activation of the PI3K/Akt pathway can be mediated by an interaction between phospho-Y737 in c-Cbl and the SH2 domains of the p85 regulatory subunit of PI3K (Thien et al., 2010), we examined the levels of phospho-Y737. Immunoblotting of lineage negative and myeloid-enriched BM cells with anti-phospho-Y737 antibodies revealed a greater fraction of the mutant c-Cbl$^{A/-}$ protein was constitutively phosphorylated on Y737 compared with WT c-Cbl (Figure 4D). This finding provides evidence that the mutant c-Cbl protein itself may be contributing to the enhanced Akt signal as previously shown in c-Cbl$^{A/-}$ thymocytes (Thien et al., 2005, 2010). Antibody specificity was confirmed by including cells from a mouse expressing a Y737F knockin mutation (i.e., F/F) that is not recognized by anti-phospho-Y737 antibodies (Thien et al., 2010).

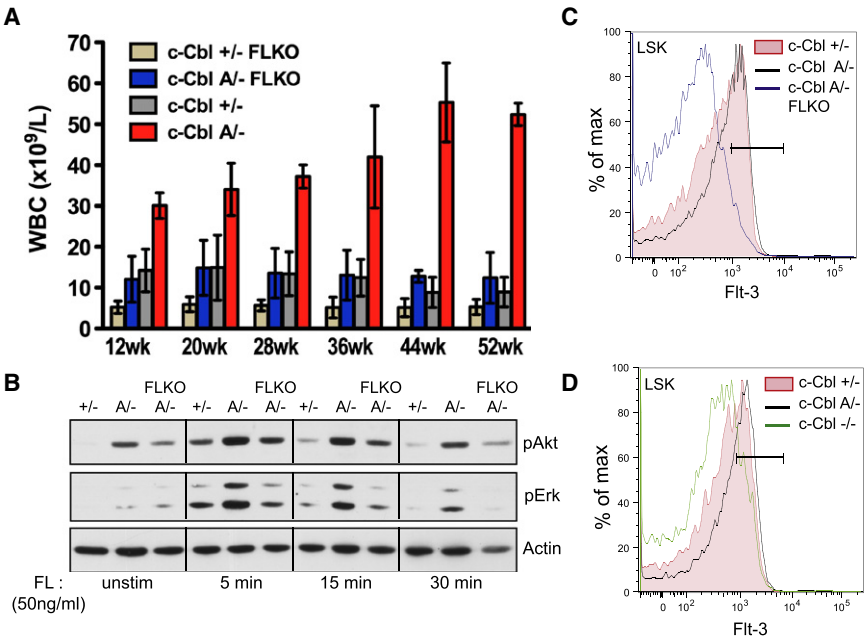

Figure 5. FL Deficiency in c-Cbl RING Finger Mutant Mice Prevents the Development of Leukemia

(A) Cohorts of c-Cbl$^{+/-}$ FLKO (n = 6), c-Cbl$^{A/-}$ FLKO (n = 7), Cbl$^{+/-}$ (n = 5), and Cbl$^{A/-}$ (n = 3) mice were bled from the tail vein at the indicated ages and WBC cells counts determined by Hemavet analysis. By 52 weeks, two of the three c-Cbl$^{A/-}$ mice had succumbed to leukemia compared with none of the c-Cbl$^{A/-}$ FLKO mice. The bar graphs represent mean WBC counts ± SD.

(B) Lineage negative BM cells from 25-week-old Cbl$^{+/-}$, Cbl$^{A/-}$, and c-Cbl$^{A/-}$ FLKO mice were left unstimulated or stimulated with FL for the indicated times. Total cell lysates were analyzed by immunoblotting with antiphospho-Akt, phospho-Erk, and actin antibodies.

(C) BM cells from 8-week-old Cbl$^{+/-}$, Cbl$^{A/-}$, and c-Cbl$^{A/-}$ FLKO mice were analyzed by flow cytometry for the cell-surface expression of FLT3 on LSK cells. Analysis of the percentages of FLT3^{high} LSK cells revealed 31%, 43%, and 5% for Cbl$^{+/-}$, Cbl$^{A/-}$, and c-Cbl$^{A/-}$ FLKO mice, respectively. The c-Cbl$^{+/-}$ FLKO littermate was also analyzed and contained 6% FLT3^{high} LSK cells indicating that the c-Cbl$^{A/-}$ mutation is unable to rescue the FLKO phenotype. See also Figure S4.

(D) BM cells from 6-week-old Cbl$^{+/-}$, Cbl$^{A/-}$, and c-Cbl$^{-/-}$ mice were analyzed by flow cytometry for the cell-surface expression of FLT3 on LSK cells. Analysis of the percentages of FLT3^{high} LSK cells revealed 33%, 50%, and 18% for Cbl$^{+/-}$, Cbl$^{A/-}$ and c-Cbl$^{-/-}$ mice, respectively. See also Figure S4.

FLT3 Ligand Deficiency Prevents the Development of Leukemia in c-Cbl$^{A/-}$ Mice

Recent studies of hematopoietic cell lines coexpressing oncogenic forms of c-Cbl and WT FLT3 have provided evidence that patients with c-Cbl mutations may benefit from FLT3 tyrosine kinase inhibitor treatment (Reindl et al., 2009; Sargin et al., 2007). In addition the findings that c-Cbl$^{A/-}$ hematopoietic progenitors show greater responsiveness to FL stimulation (Figures 4B and 4C) are consistent with this hypothesis. Here, we tested this via a genetic approach by mating c-Cbl RING finger mutant mice with FLT3 ligand-deficient mice (i.e., FLKO mice) (McKenna et al., 2000). By monitoring cohorts of double and single mutant mice, we found that the FL deficiency in c-Cbl$^{A/-}$ mice caused a marked reduction in peripheral WBC counts (Figure 5A), an effect that was evident in both the B and myeloid lineages (Figure S4). Furthermore, in striking contrast to c-Cbl$^{A/-}$ mice where two of the three mice in this cohort succumbed to leukemia by 52 weeks, none of the seven double mutant mice showed any signs of leukemia development. Analysis of liver, kidney, and lung sections at 52 weeks also revealed that the loss of FL prevented myeloid cell invasiveness (Figure S4). The FL deficiency, however, did not completely circumvent increased intrasplenic hematopoiesis and splenomegaly, although it was reduced compared with c-Cbl$^{A/-}$ mice (Figure S4). Representative FACS profiles show the extent of myeloid lineage expansion in the spleens of both c-Cbl$^{A/-}$ and c-Cbl$^{A/-}$ FLKO (Figure S4).

Constitutive activation of Akt Is Suppressed in c-Cbl$^{A/-}$ FLKO Progenitors

To determine whether the FL deficiency in c-Cbl$^{A/-}$ mice affects signaling in hematopoietic progenitors, we examined the activity of Akt and Erk. Immunoblotting of lysates from Lin$^-$ cells with phospho-Akt antibodies revealed a reduced level of constitutively active Akt in cells from c-Cbl$^{A/-}$ FLKO mice compared with c-Cbl$^{A/-}$ mice (Figure 5B). This suggests that FLT3 signaling contributes to the enhanced constitutive activation of Akt in hematopoietic progenitors from c-Cbl$^{A/-}$ mice, and that this signal may be involved in promoting the MPD. Furthermore following stimulation with FL the Lin$^-$ cells from c-Cbl$^{A/-}$ FLKO mice did not activate Akt or Erk to the levels observed in c-Cbl$^{A/-}$ cells suggesting a deficiency in a FLT3-responsive population. Indeed, examination of LSK cells from c-Cbl$^{A/-}$ FLKO mice revealed a marked reduction in cells expressing high levels of FLT3 (Figure 5C). In contrast LSK FLT3^{high} cells are expanded in c-Cbl$^{A/-}$ mice compared with cells from WT c-Cbl$^{+/-}$ mice (Figure 5C). Thus, the decreased responsiveness of c-Cbl$^{A/-}$ FLKO Lin$^-$ cells to FL stimulation compared with c-Cbl$^{A/-}$ cells appears to be due to markedly different proportions of FLT3^{high} cells. It is intriguing, however, that in spite of the low level of FLT3 expression on c-Cbl$^{A/-}$ FLKO cells the FL-induced Akt signal remains more intense compared with c-Cbl$^{+/-}$ cells which have a higher proportion of the FLT3^{high} population. Thus, the enhanced Akt signal in cells expressing the RING finger domain mutation is not solely a consequence of increased RTK levels.

c-Cbl Knockout Mice Are Deficient in FLT3^{high} LSK Cells

The finding that the prevention of leukemia in c-Cbl$^{A/-}$ FLKO mice correlates with a marked reduction in the numbers of FLT3^{high} LSK cells suggests these cells may be involved in disease development. We therefore examined whether resistance to leukemia in c-Cbl$^{-/-}$ mice may also be linked to a perturbation in FLT3^{high} LSK cells. Strikingly, we found that in c-Cbl$^{-/-}$ mice this population is markedly reduced (Figure 5D). From four

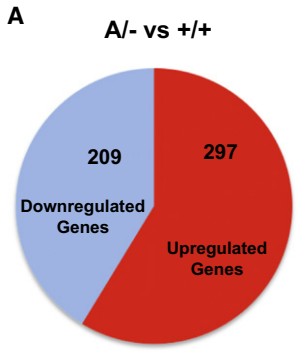

B

S.No.	GO functions	UP (#)	Down (#)	Total (#)
1	Ion Transport	11	24	35
2	Immune response	17	17	34
3	Metabolism	17	13	30
4	Protein turnover	14	14	28
5	Membrane	6	20	26
6	Chromatin modification	1	24	25
7	Signal Transduction	18	6	24
8	Transcription	14	10	24
9	Cytoskeleton/ Cell adhesion	8	10	18
10	RNA turnover	10	6	16
11	Proliferation	6	5	11
12	Differentiation	6	4	10
13	Development	2	4	6
14	Apoptosis	3	3	6
15	Communication	5	0	5
16	Chemotaxis	3	0	3

C

Upregulated

S.No.	Gene	Fold
1	Fosl2	1.8
2	Lbh	1.78
3	Per1	1.77
4	Pml	1.74
5	Id2	1.73
6	Taf6	1.73
7	Id1	1.7
8	Fos	1.67
9	Supt16h	1.67
10	Idb2	1.64
11	Hoxb5	1.57
12	Rorc	1.55
13	Meis1	1.54
14	Hes1	1.53

Downregulated

S.No.	Gene	Fold
1	Gata1	-1.58
2	Fus	-1.6
3	Runx1t1	-1.61
4	Klf2	-1.68
5	Mns1	-1.67
6	Junb	-1.7
7	Zfp367	-1.74
8	Egr1	-2.2
9	Cited4	-2.25
10	Klf1	-4.84

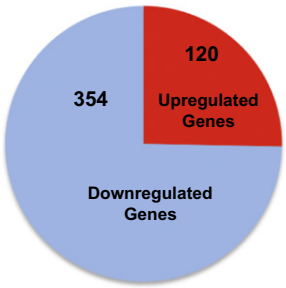

E

Upregulated

S.No.	Gene	Fold
1	Supt16h	4.36
2	Trim30	4.11
3	Twistnb	3.63
4	Taf6	2.53
5	Id2	2.17
6	Pml	2.00
7	Lbh	1.71
8	Bcl6	1.70
9	Wwtr1	1.67
10	Id1	1.63
11	Pou2af1	1.61
12	Rorc	1.61
13	Fosl2	1.55
14	Klf2	1.52

Downregulated

S.No.	Gene	Fold
1	Zfp326	-1.51
2	Ciao1	-1.51
3	Myb	-1.58
4	Zfp367	-1.71
5	JunB	-1.76

F

Subsets	A/- vs. +/+	A/- vs. +/+
	UP	DOWN
STHSC	19	156
MPP	38	293
CMP	28	76
GMP	170	198
MEP	27	251

Figure 6. Genome-wide Transcriptional Profiling Assays Identify Deregulated Expression of Genes in c-Cbl$^{A/-}$ Hematopoietic Stem and Progenitor Cells

(A) Diagram representing the total number of upregulated and downregulated genes in c-Cbl$^{A/-}$ LT-HSCs when compared with c-Cbl$^{+/+}$ LT-HSCs. Transcriptional profiling analysis was performed on highly purified (>98%) LT-HSCs obtained from the BM of 8-week-old c-Cbl$^{+/+}$ and c-Cbl$^{A/-}$ mice.

(B) The Gene Ontology (GO) analysis. Genes that were differentially expressed in LT-HSCs of c-Cbl$^{A/-}$ mice were subjected to the GO analysis to identify the major clusters of genes. Differentially expressed genes were grouped either based on their involvement in a specific biological process or based on its molecular functions. Indicated are the numbers (#) of upregulated and downregulated genes under each major category listed.

(C) List of transcription factors that were upregulated (left) and downregulated (right) in c-Cbl$^{A/-}$ LT-HSCs when compared with c-Cbl$^{+/+}$ LT-HSCs.

(D) Diagram representing the total number of upregulated and downregulated genes in c-Cbl$^{A/-}$ LT-HSCs when compared with c-Cbl$^{-/-}$ LT-HSCs.

(E) List of transcription factors that were upregulated (left) and downregulated (right) in c-Cbl$^{A/-}$ LT-HSCs when compared with c-Cbl$^{-/-}$ LT-HSCs.

(F) List of total number of upregulated and downregulated genes in ST-HSCs, MPPs, CMPs, GMPs, and MEPs of c-Cbl$^{A/-}$ mice when with to the respective progenitor subsets of c-Cbl$^{+/+}$ mice. See also Figure S5 and Tables S1–S4.

experiments analyzing young preleukemic mice, we found an average of 18.5% FLT3^{high} LSK cells in c-Cbl$^{-/-}$ mice compared with 31.5% and 50.8% in c-Cbl$^{+/-}$ and c-Cbl$^{A/-}$ mice, respectively. This finding not only further implicates this population as playing a role in the development of c-Cbl-associated leukemia but also suggests that signaling by WT c-Cbl may be involved in the generation and/or maintenance of cells with a phenotype that consistent with that of multipotent progenitors.

Transcription Profiling of c-Cbl Mutant HSCs

Intensive research in recent years has provided many clues about the biology of the transformation of HSC to leukemic stem cells (LSCs) but, nevertheless, the molecular mechanisms that promote this transformation remain poorly understood (Steidl et al., 2006). We therefore carried out a genome-wide transcriptional profiling of LT-HSCs from 8-week-old preleukemic c-Cbl$^{A/-}$ and c-Cbl$^{+/+}$ mice in an attempt to identify these molecular events. Using the Illumina microarray system, we identified 297 upregulated and 209 downregulated genes in c-Cbl$^{A/-}$ LT-HSCs when compared with LT-HSCs of c-Cbl$^{+/+}$ mice (Figure 6A; Table S1). To obtain insights into which molecular pathways are deregulated, a Gene Ontology (GO) analysis was performed. This revealed several major clusters of genes that are deregulated in c-Cbl$^{A/-}$ LT-HSCs. These include genes involved in ion transport, immune responses, metabolism, membrane proteins, protein turnover, chromatin modification, signal transduction, and transcription factors (Figure 6B; Table S2). Intriguingly, our analysis identified a remarkable bias in the downregulation of genes associated with chromatin modification compared with those that are upregulated, i.e., 24 to 1, respectively (Figure 6B; Table S2). In light of this, it is tempting to speculate that significant changes in chromatin architecture and assembly might be associated with the transformation of normal HSCs of c-Cbl$^{A/-}$ mice.

Table 1. Testing the Involvement of Individual Candidate Transcription Factors in the Development of Myeloid Leukemia

Sample No.	Candidates	Approach	No. of Cells	No. of Mice	Observation (Months)			
					3	6	9	12
1	Id1	Knockdown	500,000	10	0/10	6/10	9/10	10/10
2	Hes1	Knockdown	500,000	10	0/10	5/10	10/10	10/10
3	Fosl2	Knockdown	500,000	10	0/10	6/10	10/10	10/10
4	Pml	Knockdown	500,000	10	0/10	2/10	6/10	8/10
5	JunB	Overexpression	500,000	10	0/10	7/10	10/10	10/10
6	Klf2	Overexpression	500,000	10	0/10	5/10	8/10	10/10
7	GFP	Control	500,000	10	0/10	6/10	9/10	10/10

The expression of candidate transcription factors in c-Cbl$^{A/-}$ LT-HSCs was modulated either by shRNA-mediated knockdown (Id1, Hes1, Fosl2, Pml) or by retroviral-mediated overexpression (JunB and Klf2). Cells transduced with empty vector (IRES-GFP) served as controls. Two days after transduction, 5 × 10^5 GFP$^+$ cells were sorted and injected into sublethally irradiated *RAG2*-deficient animals. Recipients were observed and evaluated for the development of leukemia as described in Figure 3B for up to 12 months. See also Figure S6.

Transcription factors (TFs) represent the nodal point in the control of hematopoiesis (Shivdasani and Orkin, 1996) and are believed to be the master regulators that determine hematopoietic cell fate (Bonnet, 2005). Hence, we aimed to identify the TFs that are differentially expressed in c-Cbl mutant LT-HSCs. Our microarray analysis revealed 14 upregulated and 10 downregulated TFs in c-Cbl$^{A/-}$ LT-HSCs when compared with c-Cbl$^{+/+}$ LT-HSCs (Figure 6C; Tables S1 and S2). Validation by real-time quantitative PCR confirmed the differential expression of ten of the upregulated and five of the downregulated TFs (Figure S5A and S5B). Strikingly, 12 of these differentially expressed TFs, i.e., *Fosl2, Per1, Pml, Id2, Id1, Hoxb5, Rorc, Hes1, Fus, Klf2, JunB*, and *Egr1* are associated with the onset or development of hematopoietic neoplasms.

In view of the differing phenotypes between c-Cbl$^{-/-}$ and c-Cbl$^{A/-}$ mice, we hypothesized that the gene expression profiles might also be dissimilar between their LT-HSCs. Strikingly, a direct comparison between c-Cbl$^{A/-}$ and c-Cbl$^{-/-}$ LT-HSCs revealed differential expression of 474 genes (354 upregulated and 120 downregulated) (Figure 6D; Table S3) which included upregulation of 14 TFs and downregulation of 5 TFs (Figure 6E; Table S3). Interestingly, 8 of the 14 TFs, i.e., *Supt16h, Taf6, Id2, Pml, Lbh, Id1, Fosl2*, and *Rorc*, are commonly upregulated, and 2 of 5 TFs, i.e., *Zfp367* and *JunB*, are commonly downregulated in c-Cbl$^{A/-}$ LT-HSCs when compared with both c-Cbl$^{+/+}$ and c-Cbl$^{-/-}$ LT-HSCs (Figure S5). However, 13 TFs (6 upregulated and 7 downregulated) are differentially expressed in c-Cbl$^{A/-}$ cells when compared only with c-Cbl$^{+/+}$ cells (Figure S5C). Taken together, these results reveal that c-Cbl$^{A/-}$ and c-Cbl$^{-/-}$ LT-HSCs have very distinct molecular signatures and these might explain the differences in the phenotypes observed between c-Cbl$^{A/-}$ and c-Cbl$^{-/-}$ mice.

In addition, we investigated whether the deregulated gene expression observed in the LT-HSCs of c-Cbl$^{A/-}$ mice changed the expression profile of downstream progenitors. Transcriptional profiling of purified ST-HSCs, MPPs, CMPs, GMPs, and MEPs revealed that a total of 175 genes in ST-HSCs, 331 genes in MPPs, 104 genes in CMPs, 368 genes in GMPs, and 278 genes in MEPs were differentially expressed in c-Cbl$^{A/-}$ hematopoietic progenitors when compared with the same of c-Cbl$^{+/+}$ mice (Figure 6F; Table S4; data not shown).

Modulating the Expression of Individual Candidate TFs Does Not Affect c-Cbl-Directed Leukemia

To investigate whether changes in the expression of individual TFs might be essential for the c-Cbl$^{A/-}$ phenotype, we examined the effects of shRNA-mediated knockdown or retroviral-mediated overexpression of selected TFs. We chose TFs that are associated with leukemogenesis and are overexpressed in c-Cbl$^{A/-}$ LT-HSCs, such as *Pml*, *Id1, Hes1*, and *Fosl2*, as candidates for the knockdown studies and TFs that are downregulated in c-Cbl$^{A/-}$ LT-HSCs such as *JunB* and *Klf2* as candidates for overexpression studies. The effectiveness of the knockdown or overexpression of these genes and the repopulating efficiency is shown in Figure S6. Interestingly, we found that neither the knockdown nor overexpression of these TFs prevented the development of leukemia (Table 1), although knockdown of *Pml* did delay the onset (Table 1). This effect, although not profound, is of interest in light of the requirement of *Pml* for the maintenance of both HSCs and LSCs (Ito et al., 2008). These data support the notion that an array of TFs contribute to the phenotype of c-Cbl$^{A/-}$ mice; however, the targeting of these genes in isolation is unlikely to be an effective approach in retarding leukemia development.

Taken together, the transcriptional profiling data suggest that the dynamic balance of a regulatory network of many pathways is determining the leukemic transformation of normal HSCs to LSCs. Although the transcriptional profiling has identified genes that may promote a heightened probability of further genetic changes within c-Cbl$^{A/-}$ LT-HSCs, further studies are required to delineate the precise molecular control of leukemogenesis mediated by the c-Cbl RING finger mutant protein.

DISCUSSION

This study represents a detailed characterization of an in vivo model for c-Cbl-associated MPNs. We demonstrate that the c-Cbl RING finger mutant mouse permits the analysis of signaling events in hematopoietic progenitors that promote susceptibility to leukemia as well as providing a means for identifying additional genetic changes that lead to leukemia. Importantly, this mouse provides a way for testing the efficacy of compounds that target signaling pathways that are altered as a consequence of c-Cbl RING finger domain mutations.

c-Cbl was identified to function as a negative regulator of RTK signaling through genetic studies in *C. elegans* (Yoon et al., 1995) and the biochemistry was determined soon after by landmark studies identifying c-Cbl and other family members as E3 ubiquitin ligases that target RTKs (Joazeiro et al., 1999; Levkowitz et al., 1999). With the widespread involvement of RTKs in human tumorigenesis, it is surprising that a decade passed before c-Cbl mutations were found in human cancers. These cancers have so far been restricted to MPNs and more recently lung cancers (Tan et al., 2010). In this study, we characterize an MPD that invariably leads to a lethal myeloid leukemia in the c-Cbl RING finger mutant mouse. In contrast, the c-Cbl$^{-/-}$ mouse develops a mild MPD that does not lead to leukemia. This is consistent with no c-Cbl null mutations being found in human tumors. The more profound effects of retaining the mutant c-Cbl protein, as opposed to a complete loss, raises the interesting question of whether the c-Cbl mutant protein is principally functioning as a dominant negative for Cbl-b or as a constitutively active oncogene, or indeed both. Although addressing this question is beyond the scope of this study, a recent publication concluded that mutations that result in the loss of E3 ligase activity in human MPNs also result in a gain-of-function consistent with that of an oncogene (Sanada et al., 2009). While our findings here and in earlier studies are consistent with this idea, we believe that the profound phenotype of the c-Cbl RING finger mutant mouse is probably the combination of a block to Cbl-b compensation as well as the provision of a highly phosphorylated signaling platform that activates the PI3K pathway.

Given c-Cbl's role as a negative regulator of RTK signaling, it is significant that we identified FLT3 as a key component in promoting c-Cbl-associated MPD and leukemia. Activating mutations in FLT3 are common in human leukemias (Stirewalt and Radich, 2003) and WT FLT3 attains an "activated" phenotype when coexpressed with oncogenic forms of c-Cbl (Reindl et al., 2009; Sargin et al., 2007). Thus, it was encouraging that the predictions from in vitro experiments were translated to an animal model where FLT3 signaling was enhanced in hematopoietic progenitors. Consistent with this, we prevented the development of MPD and leukemia in the c-Cbl RING finger mouse by mating to FL knockout mice, thus providing credence for the use of FLT3 kinase inhibitors as a potential therapy for c-Cbl-associated leukemias. Equally hopeful may be the effectiveness of inhibitors of the PI3K pathway since a downstream consequence of enhanced FLT3 signaling by the c-Cbl mutant protein is the constitutive and sustained activation of Akt in hematopoietic progenitors.

Importantly, we also identified LT-HSCs as being the sole population of cells capable of transferring both the preleukemic MPD and the leukemic phenotype to irradiated WT recipients. In contrast, ST-HSCs and MPPs from preleukemic or leukemic mice do not have this capability. This is an intriguing finding in view of the unique phenotype of the c-Cbl RING finger mutant mouse with its expanded population of FLT3^{high} LSK cells, a phenotype that defines MPPs (Yang et al., 2005). So although this expanded population correlates with MPD and leukemia development, these cells alone are insufficient to cause disease. Nonetheless it is striking that the LSK FLT3^{high} population is reduced in both c-Cbl$^{-/-}$ mice and c-Cbl$^{A/-}$ mice on a FLKO background neither of which develop leukemia. Thus, the evidence supports a key requirement for the FLT3^{high} population in c-Cbl-directed leukemogeneis; however, the biochemical changes in these cells that are caused by the c-Cbl mutation are alone insufficient to promote a long-term repopulating capability.

An additional consequence of the c-Cbl RING finger mutation is the deregulated expression of many genes in LT-HSCs compared with genes in WT and c-Cbl$^{-/-}$ LT-HSCs. Because of the large number of genes identified, it was feasible to only focus on a select few and determine whether they play a causative role in promoting leukemia in c-Cbl RING finger mutant mice. We therefore selected transcription factors that were differentially regulated in c-Cbl$^{A/-}$ LT-HSCs compared with either c-Cbl$^{+/+}$ or c-Cbl$^{-/-}$ LT-HSCs in addition to having a known association with leukemia development. Other than a modest effect of *Pml* knockdown none of the genes, when either knocked down or overexpressed in c-Cbl$^{A/-}$ HSCs, were able to suppress the development of leukemia in transplanted recipients. Clearly, there is a limitation in these experiments to precisely revert the expression of transcription factors to WT levels; however, the results do suggest that identifying and targeting individual transcription factors with causative roles will be a difficult task. Indeed, it is more likely that a collaboration of several transcription factors and other signaling molecules are involved in promoting the heightened susceptibility to leukemia.

In conclusion, this study has provided a detailed characterization of a preclinical murine model for c-Cbl-associated MPNs and has set the stage for the use of this model to identify compounds that will provide the best possible options for effective treatments.

EXPERIMENTAL PROCEDURES

Mice

The generation of c-Cbl$^{-/-}$, c-Cbl(C379A), Cbl-b$^{-/-}$, Cbl-b(C373A), and c-Cbl (Y737F) mice have been previously described (Bachmaier et al., 2000; Murphy et al., 1998; Oksvold et al., 2008; Thien et al., 2005, 2010). FLT3 ligand knockout mice were purchased from Taconic (Hudson, NY) and were originally generated in the laboratory of Dr. Jacques Peschon (McKenna et al., 2000). For transplantation studies, *RAG2*$^{-/-}$ mice on a CD45.1 congenic background were used. All mice were maintained on a C57BL/6 background with the exception of c-Cbl$^{-/-}$ mice that were maintained on a mixed C57BL/6J x129Sv/J background. All mouse experiments were approved and performed in accordance with the guidelines and regulations of the Animal Ethics Committee at the University of Western Australia (approval 07/100/578) and the Institutional Animal Care and Use Committee of Yale University (IACUC). Mice were housed under pathogen-free conditions in microisolator cages at animal facilities at the University of Western Australia and Yale University. Mice were monitored three times per week by visual inspection and palpation and monthly by peripheral blood analysis. Blood was collected from the tail vein and white blood cell counts determined using a Beckman Coulter LH750 counter. Differential blood count analysis was performed using the Hemavet 950 LV system (DREW Scientific, Waterbury, CT). Nucleated blood cells were further characterized by phenotyping with lineage-specific antibodies and flow cytometry (see Supplemental Experimental Procedures), and blood films were stained by an automated Diff Quick procedure. Following sacrifice mice were photographed and visually examined for tumor development.

Transplantation Studies

For BM transplantation studies, 1 × 10^6 RBC lysed BM cells of either c-Cbl$^{A/+}$ or c-Cbl$^{A/-}$ mice were transplanted intravenously into lethally irradiated (11 Gy) CD45.1 congenic recipients. Alternatively, 1 × 10^6 RBC lysed BM cells of WT

CD45.1 congenic mice were transplanted into lethally irradiated c-Cbl$^{A/+}$ or c-Cbl$^{A/-}$ CD45.2 recipients. For HSC and progenitor transplantation studies, sublethally (5.5 Gy) irradiated *RAG2*$^{-/-}$ CD45.1 recipient mice were injected with fractionated donor BM subsets (see Supplemental Experimental Procedures) isolated from either 8- or 40-week-old c-Cbl$^{A/+}$ and c-Cbl$^{A/-}$ mice. Recipients were monitored monthly for up to 12 months, starting at 4 weeks after transplantation, by flow cytometric and differential blood count analyses of peripheral blood.

Immunoblotting

Lineage-negative BM cells purified using a hematopoietic progenitor cell enrichment kit (BD Biosciences) were incubated for 1 hr in serum-free IMDM medium at 37°C before stimulation with recombinant mouse SCF or FLT3 ligand (R&D Systems). The stimulation was terminated by the addition of SDS sample buffer and cell lysates examined by immunoblotting with anti-phospho-Akt(Ser473), anti-phospho-Erk1/2(T202/Y204), anti-phospho-c-Cbl (Y731) (Cell Signaling Technology), anti-c-Cbl (Upstate Biotechnology), or anti-Actin (Sigma) antibodies.

Statistical Analysis

Data are presented as mean ± SD. Statistical significance was assessed using a two-sided unpaired Student's t test. p values >0.05 were considered to be nonsignificant and p values <0.05 were considered to be significant.

Microarray Studies

Transcription profiling studies were conducted using the Illumina MouseWG-6 v2.0 BeadChips arrays (Illumina Inc., San Diego, CA) according to the manufacturer's instruction at the Keck microarray facility, Yale University. In brief, labeled cRNA for hybridization onto Illumina BeadChips was prepared using a TotalPrep RNA Amplification kit (Applied Biosystems). Double stranded cDNA and biotin-labeled cRNA were synthesized and purified from 500 ng of total RNA. cRNA was purified and the integrity of cRNA was assessed by running aliquots on the Bioanalyzer prior to hybridization. Hybridization buffer from the BeadChip kit (Illumina) was mixed with 1500 ng of biotin-labeled cRNA, heated to 65°C for 5 min, and then loaded onto the BeadChip. After hybridization at 58°C for 16–20 hr, the BeadChips were washed and stained in a series of washes and stains as outlined in the Illumina protocol. Finally, the BeadChips were scanned on the Illumina BeadArray Reader and analyzed using the BeadStudio software. Quality control parameters were checked for all arrays and the data normalized for background. The Gene Ontology (GO) analysis was performed using the Gene spring GX (Agilent Technologies) and the online AmiGO (AmiGO Version: 1.7) software. Differentially expressed genes were classified under major trees based on their molecular functions.

ACCESSION NUMBERS

The microarray data have been deposited in NCBI GEO under accession number GSE23564.

SUPPLEMENTAL INFORMATION

Supplemental Information includes Experimental Procedures, six figures, and four tables and can be found online at doi:10.1016/j.ccr.2010.09.008.

ACKNOWLEDGMENTS

This work was supported by NHMRC Project Grants 572516 and 634414, NHMRC Research Fellowship 303112 (Canberra), and the MHRIF (Health Department of W. Australia). We thank Samantha Dagger for mouse genotyping, Slavica Pervan for preparing histopathology sections, and Jill Finlayson and John Papadimitriou for help with leukemia diagnosis. We acknowledge the support of the Yale Cell Sorter Facility and the Keck Microarray facility, Yale University. R.A.F. is an investigator of Howard Hughes Medical Institute. C.R. is funded by a grant from the Bill and Melinda Gates foundation through the Grand Challenges in Global Health initiative.

Received: March 4, 2009
Revised: July 7, 2010
Accepted: August 19, 2010
Published: October 18, 2010

REFERENCES

Abbas, S., Rotmans, G., Lowenberg, B., and Valk, P.J.M. (2008). Exon 8 splice site mutations in the gene encoding the E3-ligase *CBL* are associated with core binding factor acute myeloid leukemias. Haematologica *93*, 1595–1597.

Bachmaier, K., Krawczyk, C., Kozieradzki, I., Kong, Y.-Y., Sasaki, T., Oliveira-dos-Santos, A., Mariathasan, S., Bouchard, D., Wakeham, A., Itie, A., et al. (2000). Negative regulation of lymphocyte activation and autoimmunity by the molecular adaptor Cbl-b. Nature *403*, 211–216.

Bandi, S.R., Brandts, C., Rensinghoff, M., Grundler, R., Tickenbrock, L., Kohler, G., Duyster, J., Berdel, W.E., Muller-Tidow, C., Serve, H., and Sargin, B. (2009). E3 ligase-defective Cbl mutants lead to a generalized mastocytosis and myeloproliferative disease. Blood *114*, 4197–4208.

Bonnet, D. (2005). Normal and leukemic stem cells. Br. J. Haematol. *130*, 469–479.

Caligiuri, M.A., Briesewitz, R., Yu, J., Wang, L., Wei, M., Arnoczky, K.J., Marburger, T.B., Wen, J., Perrotti, D., Bloomfield, C.D., and Whitman, S.P. (2007). Novel c-CBL and CBL-b ubiquitin ligase mutations in human acute myeloid leukemia. Blood *110*, 1022–1024.

Dunbar, A.J., Gondek, L.P., O'Keefe, C.L., Makishima, H., Rataul, M.S., Szpurka, H., Sekeres, M.A., Wang, X.F., McDevitt, M.A., and Maciejewski, J.P. (2008). 250K single nucleotide polymorphism array karyotyping identifies acquired uniparental disomy and homozygous mutations, including novel missence substitutions of c-Cbl in myeloid malignancies. Cancer Res. *68*, 10349–10357.

Grand, F.H., Hidalgo-Curtis, C., Ernst, T., Zoi, K., Zoi, C., McGuire, C., Kreil, S., Jones, A., Score, J., Metzgeroth, G., et al. (2009). Frequent Cbl mutations associated with 11q acquired uniparental disomy in myeloproliferative neoplasms. Blood *113*, 6182–6192.

Ito, K., Bernardi, R., Morotti, A., Matsuoka, S., Saglio, G., Ikeda, Y., Rosenblatt, J., Avigan, D.E., Teruya-Feldstein, J., and Pandolfi, P.P. (2008). PML targeting eradicates quiescent leukaemia-initiating cells. Nature *453*, 1072–1078.

Joazeiro, C.A.P., Wing, S.S., Huang, H.-K., Leverson, J.D., Hunter, T., and Liu, Y.-C. (1999). The tyrosine kinase negative regulator c-Cbl as a RING-type, E2-dependent ubiquitin-protein ligase. Science *286*, 309–312.

Kales, S.C., Ryan, P.E., Nau, M.M., and Lipkowitz, S. (2010). Cbl and human myeloid neoplasms: the Cbl oncogene comes of age. Cancer Res. *70*, 4789–4794.

Langdon, W.Y., Hartley, J.W., Klinken, S.P., Ruscetti, S.K., and Morse, H.C., III. (1989). v-*cbl*, an oncogene from a dual-recombinant murine retrovirus that induces early B-lineage lymphomas. Proc. Natl. Acad. Sci. USA *86*, 1168–1172.

Lapidot, T., Sirard, C., Vormoor, J., Murdoch, B., Hoang, T., Caceres-Cortes, J., Minden, M., Paterson, B., Caligiuri, M.A., and Dick, J.E. (1994). A cell initiating human acute myeloid leukaemia after transplantation into SCID mice. Nature *367*, 645–648.

Levkowitz, G., Waterman, H., Ettenberg, S.A., Katz, M., Lavi, S., Iwai, K., Reiss, Y., Ciechanover, A., Lipkowitz, S., and Yarden, Y. (1999). Ubiquitin ligase activity and tyrosine phosphorylation underlie suppression of growth factor signaling by c-Cbl/Sli-1. Mol. Cell *4*, 1029–1040.

Loh, M.L., Sakai, D.S., Flotho, C., Kang, M., Fliegauf, M., Archambeault, S., Mullighan, C.G., Chen, L., Bergstraesser, E., Bueso-Ramos, C.E., et al. (2009). Mutations in CBL occur frequently in juvenile myelomonocytic leukemia. Blood *114*, 1859–1863.

Maciejewski, J.P., Tiu, R.V., and O'Keefe, C. (2009). Application of array-based whole genome scanning technologies as a cytogenetic tool in haematological malignancies. Br. J. Haematol. *146*, 479–488.

Makishima, H., Cazzolli, H., Szpurka, H., Dunbar, A., Tiu, R., Huh, J., Muramatsu, H., O'Keefe, C., Hsi, E., Paquette, R.L., et al. (2009). Mutations of E3

ubiquitin ligase Cbl family members constitute a novel common pathogenic lesion in myeloid malignancies. J. Clin. Oncol. *27*, 6109–6116.

Masashi, S., Yung, S.L., Suzuki, T., Kato, M., Sakata, M.Y., Kumano, K., Kawamata, N., Takita, J., Mori, H., Kurokawa, M., et al. (2008). Genome-wide analysis of MDS/MPD disclosed frequent homozygous C-Cbl mutations tightly associated with 11q-UPD. ASH Annu. Meet. Abstr. *112*, 855.

McKenna, H.J., Stocking, K.L., Miller, R.E., Brasel, K., De Smedt, T., Maraskovsky, E., Maliszewski, C.R., Lynch, D.H., Smith, J., Pulendran, B., et al. (2000). Mice lacking flt3 ligand have deficient hematopoiesis affecting hematopoietic progenitor cells, dendritic cells, and natural killer cells. Blood *95*, 3489–3497.

Muramatsu, H., Makishima, H., Jankowska, A.M., Cazzolli, H., O'Keefe, C., Yoshida, N., Xu, Y., Nishio, N., Hama, A., Yagasaki, H., et al. (2010). Mutations of an E3 ubiquitin ligase c-Cbl but not TET2 mutations are pathogenic in juvenile myelomonocytic leukemia. Blood *115*, 1969–1975.

Murphy, M.A., Schnall, R.G., Venter, D.J., Barnett, L., Bertoncello, I., Thien, C.B.F., Langdon, W.Y., and Bowtell, D.D.L. (1998). Tissue hyperplasia and enhanced T cell signalling via ZAP-70 in c-Cbl deficient mice. Mol. Cell. Biol. *18*, 4872–4882.

Naramura, M., Kole, H.K., Hu, R.-J., and Gu, H. (1998). Altered thymic positive selection and intracellular signals in Cbl-deficient mice. Proc. Natl. Acad. Sci. USA *95*, 15547–15552.

Ogawa, S., Sanada, M., Shih, L.Y., Suzuki, T., Otsu, M., Nakauchi, N., and Koeffer, H.P. (2010). Gain-of-function c-Cbl mutations associated with uniparental disomy of 11q in myeloid neoplasms. Cell Cycle *9*, 1051–1056.

Oksvold, M.P., Dagger, S.A., Thien, C.B.F., and Langdon, W.Y. (2008). The Cbl-b RING finger domain has a limited role in regulating inflammatory cytokine production by IgE-activated mast cells. Mol. Immunol. *45*, 925–936.

Owaidah, T.M., Al Beihany, A., Iqbal, M.A., Elkum, N., and Roberts, G.T. (2006). Cytogenetics, molecular and ultrastructural characteristics of biphenotypic acute leukemia identified by the EGIL scoring system. Leukemia *20*, 620–626.

Passegue, E., Wagner, E.F., and Weissman, I.L. (2004). JunB deficiency leads to a myeloproliferative disorder arising from hematopoietic stem cells. Cell *119*, 431–443.

Raaijmakers, M.H., Mukherjee, S., Guo, S., Zhang, S., Kobayashi, T., Schoonmaker, J.A., Ebert, B.L., Al-Shahrour, F., Hasserjian, R.P., Scadden, E.O., et al. (2010). Bone progenitor dysfunction induces myelodysplasia and secondary leukaemia. Nature *464*, 852–857.

Rathinam, C., Thien, C.B., Langdon, W.Y., Gu, H., and Flavell, R.A. (2008). The E3 ubiquitin ligase c-Cbl restricts development and functions of hematopoietic stem cells. Genes Dev. *22*, 992–997.

Reindl, C., Quentmeier, H., Petropoulos, K., Grief, P.A., Benthaus, T., Argiropoulos, B., Mellert, G., Vempati, S., Duyster, J., Guske, C., et al. (2009). CBL exon8/9 mutants activate the Flt3 pathway and cluster in core binding factor/11q deletion acute myeloid leukemia/myelodysplastic syndrome subtypes. Clin. Cancer Res. *15*, 2238–2247.

Rodrigues, M.S., Reddy, M.M., Walz, C., Salgia, R., Podar, K., Band, H., Reiter, A., Griffin, J.D., and Sattler, M. (2008). Novel transforming mutations of CBL in human acute myeloid leukemia. ASH Annu. Meet. Abstr. *112*, 2948.

Sanada, M., Suzuki, T., Shih, L.-Y., Otsu, M., Kato, M., Yamazaki, S., Tamura, A., Honda, H., Sakata-Yanagimoto, M., Kumano, K., et al. (2009). Gain-of-function of mutated C-CBL tumour suppressor in myeloid neoplasms. Nature *460*, 904–908.

Sargin, B., Choudhary, C., Crosetto, N., Schmidt, M.H.H., Rensinghoff, C.T., Tickenbrock, L., Schwable, J., Brandts, D.A., Koschmieder, S., Bandi, S.R., et al. (2007). Flt3-dependent transformation by inactivating c-Cbl mutations. Blood *110*, 1004–1012.

Schmidt, M.H., and Dikic, I. (2005). The Cbl interactome and its functions. Nat. Rev. Mol. Cell Biol. *6*, 907–919.

Shivdasani, R.A., and Orkin, S.H. (1996). The transcriptional control of hematopoiesis. Blood *87*, 4025–4039.

Slape, C., Liu, L.Y., Beachy, S., and Aplan, P.D. (2008). Leukemic transformation in mice expressing a NUP98-HOXD13 transgene is accompanied by spontaneous mutations in Nras, Kras and Cbl. Blood *112*, 2017–2019.

Steidl, U., Rosenbauer, F., Verhaak, R.G., Gu, X., Ebralidze, A., Otu, H.H., Klippel, S., Steidl, C., Bruns, I., Costa, D.B., et al. (2006). Essential role of Jun family transcription factors in PU.1 knockdown-induced leukemic stem cells. Nat. Genet. *38*, 1269–1277.

Stirewalt, D.G., and Radich, J.P. (2003). The role of FLT3 in haemopoietic malignancies. Nat. Rev. Cancer *3*, 650–665.

Tan, Y.H., Krishnaswamy, S., Nandi, S., Kanteti, R., Vora, S., Onel, K., Hasina, R., Lo, F.Y., El-Hashani, E., Cervantes, G., et al. (2010). CBL is frequently altered in lung cancers: its relationship to mutations in MET and EGFR tyrosine kinases. PLoS One *5*, e8972. 10.1371/journal.pone.0008972.

Thien, C.B.F., and Langdon, W.Y. (2005). c-Cbl and Cbl-b ubiquitin ligases: substrate diversity and the negative regulation of signalling responses. Biochem. J. *391*, 153–166.

Thien, C.B.F., Walker, F., and Langdon, W.Y. (2001). Ring finger mutations that abolish c-Cbl-directed polyubiquitination and downregulation of the EGF receptor are insufficient for cell transformation. Mol. Cell *7*, 355–365.

Thien, C.B.F., Scaife, R.M., Papadimitriou, J.M., Murphy, M.A., Bowtell, D.D.L., and Langdon, W.Y. (2003). A mouse with a loss-of-function mutation in the c-Cbl TKB domain shows perturbed thymocyte signaling without enhancing the activity of the ZAP-70 tyrosine kinase. J. Exp. Med. *197*, 503–513.

Thien, C.B.F., Blystad, F.D., Zhan, Y., Lew, A.M., Voigt, V., Andoniou, C.E., and Langdon, W.Y. (2005). Loss of c-Cbl RING finger function results in high-intensity signaling and thymic deletion. EMBO J. *24*, 3807–3819.

Thien, C.B.F., Dagger, S.A., Steer, J.H., Koentgen, F., Jansen, E.S., Scott, C.L., and Langdon, W.Y. (2010). c-Cbl promotes T cell receptor-induced thymocyte apoptosis by activating the phosphatidylinositol 3-kinase/Akt pathway. J. Biol. Chem. *285*, 10969–10981.

Walkley, C.R., Olsen, G.H., Dworkin, S., Fabb, S.A., Swann, J., McArthur, G.A., Westmoreland, S.V., Chambon, P., Scadden, D.T., and Purton, L.E. (2007). A microenvironment-induced myeloproliferative syndrome caused by retinoic acid receptor gamma deficiency. Cell *129*, 1097–1110.

Wang, J.C., and Dick, J.E. (2005). Cancer stem cells: lessons from leukemia. Trends Cell Biol. *15*, 494–501.

Yang, L., Bryder, D., Adolfsson, J., Nygren, J., Mansson, R., Sigvardsson, M., and Jacobsen, S.E.W. (2005). Identification of Lin-Sca1+kit+CD34+Flt3-short-term hematopoietic stem cells capable of rapidly reconstituting and rescuing myeloablated transplant recipients. Blood *105*, 2717–2723.

Yokomizo, T., and Dzierzak, E. (2008). Fine-tuning of hematopoietic stem cell homeostasis: novel role for ubiquitin ligase. Genes Dev. *22*, 960–963.

Yoon, C.H., Lee, J., Jongeward, G.D., and Sternberg, P.W. (1995). Similarity of *sli-1*, a regulator of vulval development in *C. elegans*, to the mammalian proto-oncogene c-*cbl*. Science *269*, 1102–1105.

Zheng, N., Wang, P., Jeffrey, P.D., and Pavletich, N.P. (2000). Structure of a c-Cbl-UbcH7 complex: RING domain function in ubiquitin-protein ligases. Cell *102*, 533–539.